sustainability

MDPI

Article

Utilisation of Recycled Silt from Water Treatment and Palm Oil Fuel Ash as Geopolymer Artificial Lightweight Aggregate

Shi Ying Kwek and Hanizam Awang *

School of Housing, Building and Planning, Universiti Sains Malaysia, Gelugor 11800, Penang, Malaysia; sheily1999@hotmail.com
* Correspondence: hanizam@usm.my

Abstract: The global consumption of aggregate in the construction field is increasing annually, especially in concrete production. With the development of the economy and increase of the population, the demand for concrete and, therefore, a huge amount of aggregate has increased significantly. This issue is pressing and needs to be addressed. Lightweight aggregate (LWA) is one possible solution. This study investigated the potential use of artificial LWA manufactured from alkaline-activated palm oil fuel ash (POFA) with silt due to its properties and performances. Six mixes containing up to 60% silt by total weight combined with optimised activated POFA were analysed. The artificial LWA was synthesised through a pelletising and sintering process at 1150 °C. The increase in the activated POFA proportion in the mixture induced changes in the properties of artificial LWA, including the physical and mechanical properties, durability, and microstructure. The analytical results showed that all of the artificial aggregates were categorised as LWA, based on BS EN 13055. The artificial LWA with 40% activated POFA and 60% silt had the highest crushing strength and acceptable properties for construction applications. This study summarised the performances of the final products and highlighted the different uses of imported silt and POFA as building materials for minimising environmental impacts.

Keywords: lightweight aggregate; sustainability; POFA; silt; properties

check for updates

Citation: Kwek, S.Y.; Awang, H. Utilisation of Recycled Silt from Water Treatment and Palm Oil Fuel Ash as Geopolymer Artificial Lightweight Aggregate. *Sustainability* **2021**, *13*, 6091. https://doi.org/10.3390/su13116091

Academic Editors: Serdar Durdyev, Amir Mahdiyar and Syuhaida Ismail

Received: 7 April 2021
Accepted: 25 May 2021
Published: 28 May 2021

Publisher's Note: MDPI stays neutral with regard to jurisdictional claims in published maps and institutional affiliations.

Copyright: © 2021 by the authors. Licensee MDPI, Basel, Switzerland. This article is an open access article distributed under the terms and conditions of the Creative Commons Attribution (CC BY) license (https://creativecommons.org/licenses/by/4.0/).

1. Introduction

The annual consumption of concrete by the construction industry worldwide has reached 1.6 billion tonnes of ordinary Portland cement (OPC), 10 billion tonnes of sand and rock, and 1 billion tonnes of water, thus making the concrete industry the largest consumer of natural resources on the planet [1]. It was reported that the concrete industry consumes about nine billion natural aggregates annually [2]. The high demand for concrete for building construction contributes to the embodied energy consumption and carbon dioxide (CO_2) emissions released during the production of cement. CO_2 is the most important greenhouse gas (GHG), and it is increasing in the atmosphere. It is responsible for around 70% of the greenhouse effect, which can lead to a thicker thermal blanket, thus affecting the Earth's atmosphere [3]. The exhaustion of natural resources is also an environmentally damaging factor. Hainin et al. [4] highlighted that the continuous use of natural aggregates will cause their depletion in the future. A continuous decline in granite aggregate production would affect the cost of concrete production [5]. This phenomenon has prompted many researchers to switch direction towards the utilisation of waste materials, such as fly ash, wood waste ash, slag, silica fume, and palm oil ash in the production of concrete. The use of waste materials in concrete can reduce the cost and the negative environment effects related to concrete production.

Recycling and reusing natural wastes as sustainable construction materials not only appears to be viable solution to the pollution problem, but also could be an economical option for designing green buildings. One of the approaches for reducing greenhouse

emissions in buildings is constructing energy-efficient materials using lightweight concretes that are produced using waste products. It has been found that there are many advantages of reducing the self-weight of construction. One of the methods is using lightweight concrete. Lightweight aggregate (LWA) has been found to be a contributing factor in the production of lighter concrete.

The utilisation of industrial waste products in artificial aggregate production has been deeply investigated to find wastes that can be modified into construction materials. The raw material for LWA can be of a different origin, such as sewage sludge, water treatment sludge (WTS), washing aggregate sludge, waste glass, palm oil fuel ash (POFA), fly ash, or natural raw materials (e.g., clay or slate). Silt from WTS and POFA is a type of waste material and can be utilised in concrete production.

WTS residue production is expected to increase annually, given that water treatment plants need to treat more water to fulfil the needs of the population. Two common methods, namely soil application and landfilling, can be used to dispose WTS [6]. Before disposing WTS, some of the treatment involves removing the chemical contents of WTS after a process of chemical coagulation, sedimentation, and filtration [7]. In recent years, studies have been carried out by various researchers to investigate the use of silt as a construction material. These include laboratory and full-scale attempts to use waterwork sludge as a component in the manufacturing of several materials, such as concrete, cement mortars, clay materials, and fired ceramic products (e.g., bricks, pipes, and tiles) [8]. Modifying sludge into brick has been studied and found to be a potential substitute to be used in high-temperature treatments, given that its chemical compositions are similar to those of clay [9–11]. Recycling sludge as an innovative material for LWA production can enhance the oxidation–reduction reaction, can reduce the density of LWA, and can save energy for relevant treatments. The use of the clay group as an artificial aggregate can reduce the emission of carbon dioxide, which is emitted at a rate of 0.22 tonnes per tonne of natural aggregates. Fundamentally, such approaches offer two distinct advantages: Economic savings in terms of the overall treatment plant operation costs and environmental sustainability.

POFA is a by-product generated by the incineration of palm oil shells and palm oil empty fruit bunch at 800 °C to 1000 °C, where the heating source is a mill's boiler, instead of conventional fuels. Various unwanted wastes are generated in the burning process of palm oil [12,13]. Around 5% ash is produced by weight through the incineration of solid fuels in the heating process. POFA is among the residue wastes produced after the production process is complete. A total of 0.06 million tonnes of POFA waste is estimated to be generated annually, and this situation raises the issue of disposal [7,14]. Another issue associated with the huge amounts of waste produced is its environmental effects. Due to the small particle size of ash, it can be easily carried away and can create smog on a humid day. Additionally, it affects the groundwater when seepage occurs in landfills. POFA is considered pozzolan but not cementitious. POFA has good pozzolanic properties based on the chemical analysis of X-ray fluorescence (XRF) and belongs in between Class-C and Class-F, according to ASTM C618. It can be used as a cement substitute, partial replacement, or additive in cement concrete. POFA is considered a pozzolanic material due to its rich silica content [15,16]. Consequently, industrial palm oil residue wastes have been explored to minimise the effect on the environment and to maximise the innovation in transforming wastes as useful materials.

Artificial LWAs are used in many applications, such as lightweight concrete, bricks, and insulation material for road construction. LWA has exhibited a loose bulk density of less than 1200 kg/m^3 and an oven-dried density of not more than 2000 kg/m^3 [7]. The strength of lightweight concrete is influenced by the properties of the utilised LWA. Thus, improving and modifying artificial aggregate in terms of its mechanical properties are essential for bringing about a better concrete performance. Furthermore, several aspects affect the characteristics of artificial LWA, including different manufacturing protocols or curing methods (autoclaving, cold bonding, geopolymerisation, and sintering) and pelletisation approaches. Sintering or firing is the most common process for enhancing the strength of

pellets. The sintering method is based on atomic diffusion, which is commonly applied for the mass production of lightweight products. Combination treatment approaches can also be applied, depending on the materials used. For the sintering method, the formation of a viscous mineral matrix is accepted, but the total melting conditions should not be reached [17].

The use of an alkaline activator as a stimulator is one method for improving LWA production. An alkaline activator is widely obtained from the geopolymer as it activates the geopolymerisation reaction. It reacts with the aluminium and silicate oxides existing in any raw material to form geopolymer cement [18,19]. The suitability of the alkaline-activated geopolymer is affected by the type of alkaline activator, concentration, ratio with raw geopolymer, curing method, and regime [20,21].

This study examined the feasibility of manufacturing artificial LWA from the geopolymer POFA with silt and the performances of these combinations as artificial LWA. The optimal result of alkaline-activated POFA and sintering temperature for the production of artificial LWA was determined through a preliminary experiment. The physical and chemical structures of the primary materials were investigated. Several laboratory testing methods were also applied to assess the performance of the artificial pellets in terms of their physical and mechanical properties, durability, and microstructure.

2. Materials and Methods

2.1. Raw Materials Used

The POFA was a by-product obtained from the residual burning of palm oil kernel shell and fibre at a high temperature above 1000 °C, which were collected from a palm oil mill. The collected POFA was oven-dried to remove the extra moisture content and then sieved through a 300 μm sieve to remove large unwanted coarse particles. The WTS was obtained from the residue of a water treatment plant. The sludge was dried under sunlight, the large-size residues were crushed into a small size, and the resulting residues were ground into silt. The POFA and small-sized sludge were ground into fine powders of 45 and 150 μm, respectively.

The alkaline activator for POFA geopolymer was a combination of 12 M NaOH and Na_2SiO_3. The alkaline was used to activate the POFA for forming activated POFA geopolymer. The NaOH molarity for this study was based on the recommendations of prior related studies [22,23], which were also proved to be applicable for POFA geopolymer [24,25]. The concentration of alkaline is directly proportional to the compressive strength. However, this parameter will decrease the strength properties as the molarity exceeds the limit of Na ions to react with elements within the raw material used. The effect of the alkaline concentration on geopolymer is less significant compared to that of the other factors, such as the alkaline ratio and alkaline-to-raw ratio [25,26]. NaOH was in the solute form of Formosoda-P NaOH (reagent grade, with a 99% purity), whereas Na_2SiO_3 was in liquid form. The specifications of Na_2SiO_3 and NaOH are displayed in Tables 1 and 2. Both alkaline types were industrial grade and exhibited a stable performance.

Table 1. Physical properties of the raw materials.

Materials	Specific Gravity	Specific Surface Area (m^2/g)	D_{50} (μm)	Liquid Limit (%)	Plastic Limit (%)	Plasticity Index
POFA	2.46	1.71	5.01	-	-	-
Silt	2.09	2.64	57.2	69.2	44.5	24.7
NaOH	1.53	-	-	-	-	-
Na_2SiO_3	1.40	-	-	-	-	-

Table 2. Oxide content and other chemical constituents of raw materials.

Material	Chemical Oxides (% by Total Mass)									Flux (%)	LOI (%)
	SiO_2	Al_2O_3	Fe_2O_3	MgO	CaO	Na_2O	K_2O	SO_3	Cl		
POFA	54.98	3.27	3.96	5.02	10.77	0.40	9.50	4.09	1.78	29.65	5.6
Silt	43.26	28.50	6.98	0.44	0.14	bdl	1.70	nd	nd	9.26	3.3
NaOH	-	-	-	-	-	-	-	-	-	-	-
Na_2SiO_3	30.10	-	-	-	-	9.40	-	-	-	-	-

Note: bdl = below detection limit; nd = not detected; LOI = loss of ignition.

2.2. Characteristics of Materials

The analysis of the physical properties of the raw materials, such as particle size analysis, specific gravity, and soil classification for silt, is presented in Table 1. The grind POFA contained 90% fine particles of 35 μm and medium particles (D_{50}) of 5.01 μm. The silt resulted in 50% particles with a size of 57.2 μm. This result showed that silt had a fine grain size in nature after grinding. The plastic limit, plasticity index, and liquid limit of silt were 44.49%, 24.71%, and 69.20%, respectively. The silt was considered inorganic silt, with a high compressibility, according to the Burmister classification (1949). The alkaline activator used was NaOH and Na_2SiO_3, and the specifications are shown in Table 1. NaOH was in pellet form, with a 99% purity and molecular weight of 40 g/mol, and it was fully water soluble.

The chemical and mineralogical compositions of the raw materials were investigated through XRF, X-ray diffraction (XRD), and scanning electron microscopy (SEM). As shown in Table 2, the main chemical composition of POFA and silt was silica oxide (SiO_2), and their contents were 54.98% and 43.26%. This finding was further confirmed by the result shown in Figure 1 through XRD analysis. Both materials had a high reactive silica content, which contributed to their strength ratio. Furthermore, the content of SiO_2 enhanced the formation of the 3D silica structure for the artificial LWA when sintering. POFA was categorised as a Class-C pozzolan material, according to ASTM C618-05, because it contained 10.77% of CaO and had a sum of 62.21% oxide compounds in silica, aluminium, and iron oxides ($SiO_2 + Al_2O_3 + Fe_2O_3$). It was also classified as a siliceous material. Thus, POFA enhanced the calcium–silicate–hydrate (C-S-H) gel formation by reacting silica within itself and silts to achieve a high strength. The reason was that the formation of the C-S-H gel helped to boost the hydration process. The high contents of SiO_2 and Al_2O_3 present in silt indicated that it was acidic oxide. It was also suitable for use as a binding and filling agent to make a water-permeable material with comparable engineering properties [27]. The magnesium oxide (MgO) and CaO contents for silt were low due to the absence of the carbonate mineral. The silica/alumina ratio (SiO_2/Al_2O_3) for silt was 1.52. The available fluxing elements, such as Fe_2O, MgO, CaO, sodium oxide (Na_2O), and potassium oxide (K_2O), confirmed the development of high-temperature glassy phases with a sufficient viscosity. The chemical composition of the flux for raw materials satisfied the requirement stated by Riley (1950) within the range of 4.5–31%.

The loss of ignition (LOI) of the POFA and silt were 5.6% and 3.3%, respectively. LOI could predict the amount of gas that needs to be released to perform the expanded aggregate. The LOI of POFA was mainly attributed to the oxidation of organic material. The LOI of POFA fulfilled the requirement of ASTM C618. The low LOI of POFA revealed some improvement, given that some little unburnt residues existed, which were eliminated when sintering was applied. The LOI of silt was due to the dewatering of the absorbed water or the dehydroxylation of the silt mineral at a certain temperature, such as kaolinite [28].

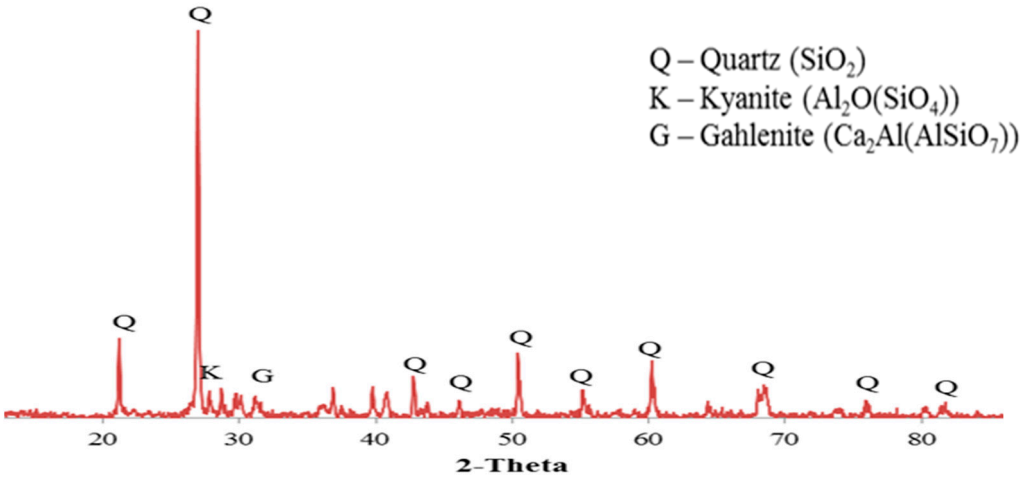

(**a**)

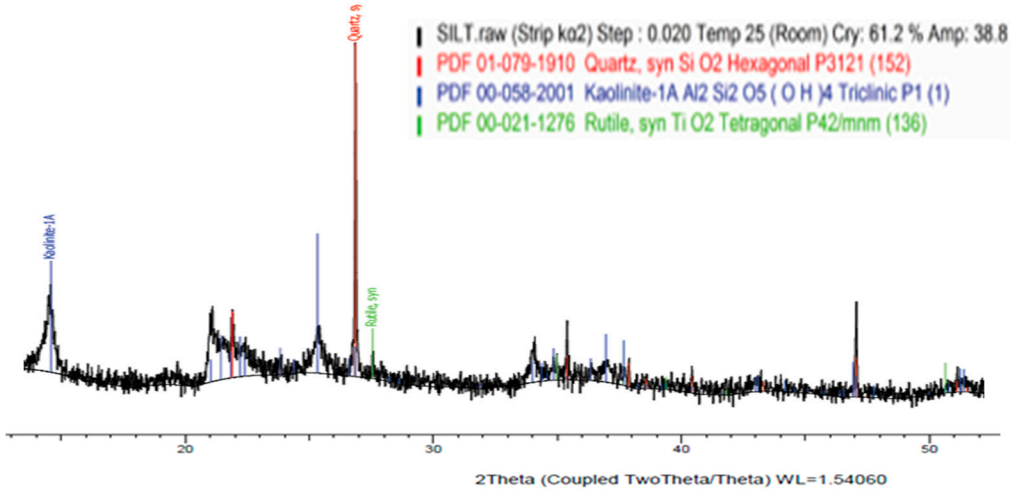

(**b**)

Figure 1. XRD pattern of (**a**) POFA and (**b**) silt.

XRD was used to determine the crystalline phase of the raw materials, as shown in Figure 1a,b. Significant quartz (SiO_2) was observed for POFA and silt. This finding could be verified by the chemical composition result, as shown in Table 2. The treated POFA was expected to have a greater strength due to the high silica content. The main minerals revealed in the matrix of POFA included quartz (SiO_2), kyanite ($Al_2O(SiO_4)$), and gahlenite ($Ca_2Al(AlSiO_2)$). The major synthesised crystalline phases within silt included quartz (SiO_2), kaolinite ($Al_2Si_2O_5(OH)_4$), and rutile (TiO_2). The presence of kaolinite contributed to the plasticity index of the silt.

The microstructures of silt and POFA particles are shown in Figure 2. The particles in POFA were small and crushed in size and shape, compared with those in the unground POFA. The particles in the ground POFA were less porous. As the size was reduced, the ground POFA particle became irregular and gained a crushed shape in its microstructure [29]. Figure 2a shows the SEM of POFA particles with an irregular arrangement, small size, and less porous appearance. This sample revealed an uneven filler particle with few and concentrated fine particles. It showed a nonuniform distribution with fracture and pebble-shaped particles. The SEM of silt presented numerous roughly angular spherical particles (Figure 2b). The cenosphere showed an acicular structure and gave a needle plate-like structure, with some angular particles. This morphology of particle allowed silt

to act as a lubricant in the interstitial space [30]. Both were varied in structure and thus had a high probability of mixing together homogeneously.

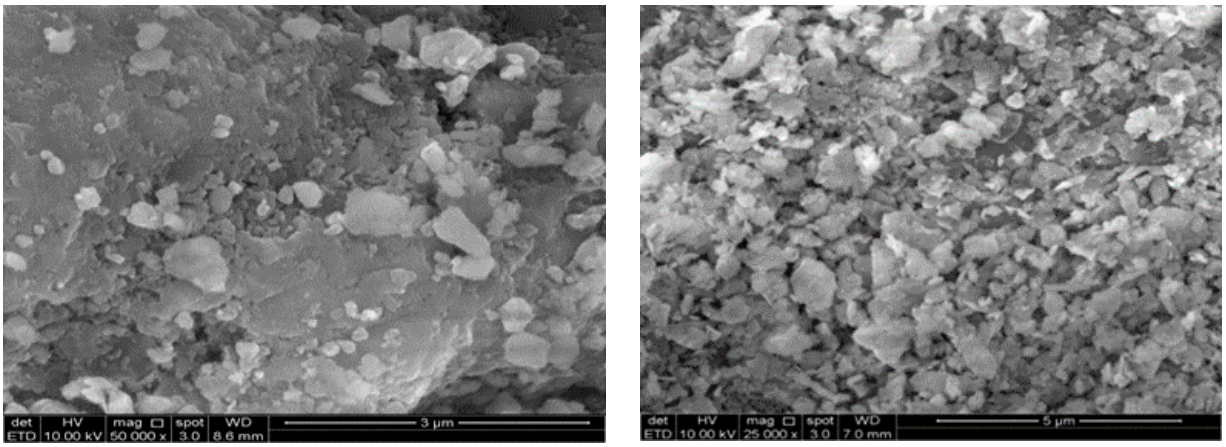

(**a**) (**b**)

Figure 2. Microstructure of (**a**) POFA and (**b**) silt.

2.3. Manufacturing of Lightweight Artificial Aggregate

The mixing proportions of artificial aggregate are shown in Table 3. For each of the mixes, character P denoted POFA, and S denoted silt. P0S10 was the control mix, which fully utilised silt without POFA. P1S9 was mixed with 10% POFA and 90% silt. There was a 10% interval increment for POFA up to 60%, which represented P6S4, based on the preliminary work. There were, in total, seven mixes in this study. The alkaline activator was prepared 1 day before mixing to ensure the homogeneous mixing of the materials.

Table 3. Mix design of raw materials for artificial aggregate production.

Mix	POFA (g)	Silt (g)	Alkaline Activator (g)		Lime (g)	Water (g)
			Na_2SiO_3	NaOH		
P0S10	-	2000.0	-	-	-	1384.0
P1S9	180.0	1800.0	85.7	34.3	20.0	1245.6
P2S8	360.0	1600.0	171.4	68.6	40.0	1107.2
P3S7	540.0	1400.0	257.1	102.9	60.0	968.8
P4S6	720.0	1200.0	342.9	137.1	80.0	830.4
P5S5	900.0	1000.0	428.6	171.4	100.0	692.0
P6S4	1080.0	800.0	514.3	205.7	120.0	553.6

These series were designed to determine the properties of artificial aggregate by varying the proportion of POFA from 0% to 60%. The mixture of Na_2O/SiO_2 in a molar ratio of 2.5 was added to POFA and lime to act as the cementitious material for silt to produce artificial aggregate. The applied optimised parameter for artificial LWA production is summarised in Table 4.

Table 4. Parameters used in the production of artificial LWA.

Parameters	Description
Liquid to solid ratio, L/S	0.6
Alkaline activator ratio, Na_2SiO_3/NaOH	2.5
Lime content (% binder weight)	10
Water for silt (% silt weight)	69.2
Curing regime	Room temperature (24 ± 2 h), followed by oven curing at 75 °C (24 ± 2 h)
Sintering regime	Preheating to 400 °C (20 min), followed by sintering at 1150 °C (1 h)

Figure 3 illustrates the manufacturing procedures for artificial LWA. First, the POFA, alkaline activator, and CaO were mixed based on the optimal proportion, which was previously determined in a preliminary experiment. Wet silt was prepared according to the controlled amount of water derived from the plastic limit, and mixed with POFA to ensure the elasticity of the mixture for extrusion. The wet mixture was then extruded using an extruder, cut into a cylinder of approximately 8 mm in length, and rounded into a round spherical granular particle of 10 mm diameter with a modified granulation instrument. The granulation was 1–2 min per cycle. The fresh granular samples were placed in room temperature for 1 day to allow for a homogeneity reaction and then oven-dried for an additional day before sintering. This procedure was conducted to prevent rapid drying and defects in the microstructure of the pellets [21–23]. The sintering temperature and dwelling time were based on the preliminary experiment. The pellets were preheated to 400 °C for 20 min and sintered at 1150 °C for 1 h. This process was established to avoid bursting due to excessive rapid heating [15]. Thereafter, the sintered pellets were cooled at room temperature before testing.

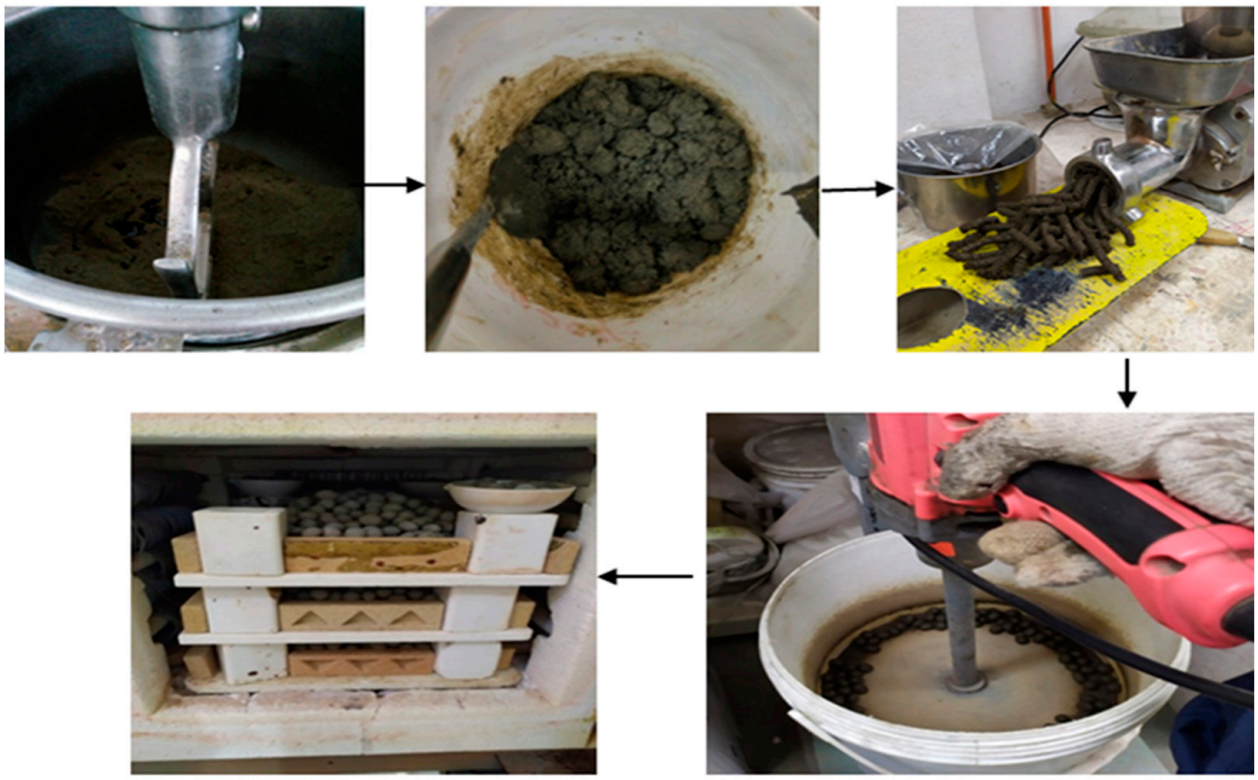

Figure 3. Process of artificial LWA manufacturing.

3. Results and Discussion

3.1. Physical Properties

As shown in Figure 4, the artificial LWAs were within 1.2 g/cm^3 and were thus categorised as LWA. The bulk density of artificial LWA increased as the proportion of activated POFA increased, and the silt content decreased. The bulk density values were within the range of 1.11–1.18 g/cm^3. The specific gravity of raw material also affected the bulk density but only slightly after the sintering. During the sintering process, the bloating index (BI) increased, which gradually decreased the grain size and the bulk density of artificial LWA [30]. The density increased, while the BI increased. This result was due to the chemical composition of artificial LWA. Specifically, some of the mineralogy substances filled the expanded void during the sintering process, which increased the bulk density.

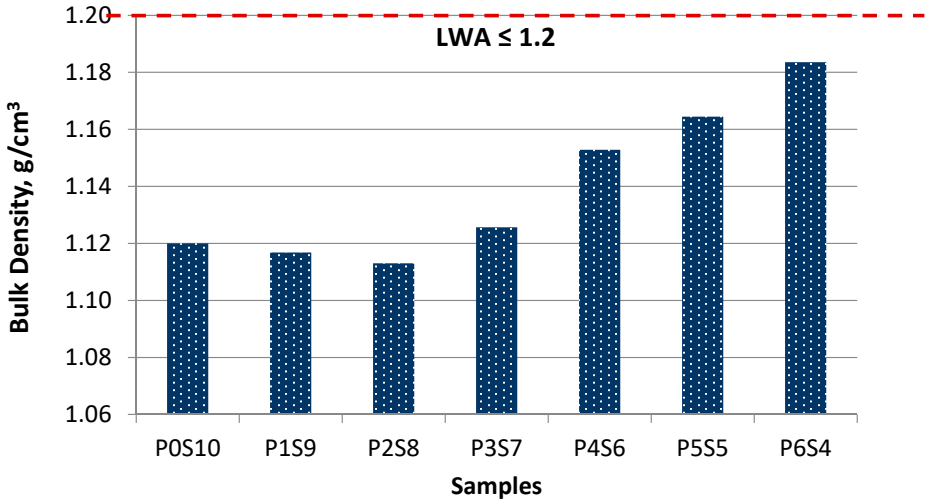

Figure 4. Performance in terms of bulk density at different ratios of activated POFA-silt artificial LWA.

The dry specific gravity of artificial LWA generally should be less than 2.0 g/cm^3, as per BS EN 13055-1-05 [30]. The specific gravity of the POFA-silt artificial aggregate in this study was 1.40–1.66 g/cm^3, as shown in Figure 5. Therefore, this material could be classified as LWA. The specific gravity and bulk density of the artificial LWA substantially changed with the increases in activated POFA and binder. Samples P0S10 to P6S4 showed an increasing trend of dry density. Sample P6S4 obtained the highest density (1.66 g/cm^3), compared with the others. This was due to the high POFA content, which caused the sample to start to melt during the sintering process. The liquid phase filled the void presence within the artificial aggregate and thus increased the aggregate density. Thus, a dense crystalline with an outer layer that had a glassy texture was generated, given that the mixture was partially melted at the sintering temperature. Therefore, these retained particles within the artificial LWA formed a closed pore structure for the interstitial voids, which led to a low water absorption and high specific gravity. Moreover, the insulated outer layer limited the accessibility of water for artificial LWA. Sample P0S10 obtained a lower dry particle density at the same sintering temperature. This low density may have been caused by the bloating phenomenon during the sintering process, which resulted in an insufficient gas evolution to form pores within the fully silt pellets. The particle density measurement showed the effect of the binder, given that the proportion of POFA to silt for artificial LWA mixtures exhibited a rising trend in terms of density. The dry particle density increased as the activated POFA content increased. As the fineness of raw materials increased, the specific gravity of manufactured artificial aggregate increased.

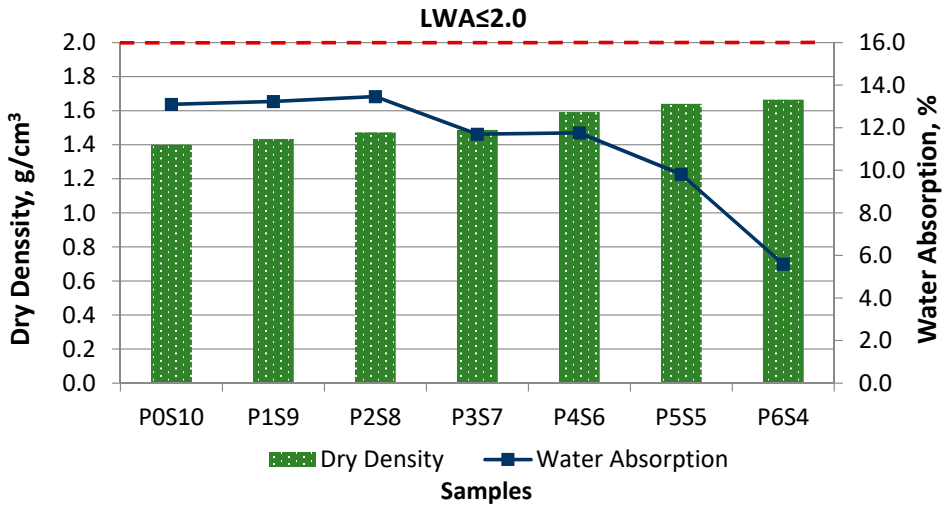

Figure 5. Relationship between dry density and water absorption at different ratios of activated POFA-silt artificial LWA.

Figure 5 shows the water absorption of artificial LWA, with values of 13.10%, 13.23%, 13.46%, 11.70%, 11.75%, 9.81%, and 5.59%, which were within the acceptable range for concrete applications. The water absorption of LWA should not be more than 20% to ensure that the mechanical properties of the aggregate are suitable for concrete production [31,32]. The water absorption, which was below 10%, indicates that the surface of the manufactured LWA was well vitrified, as per standard 10262, 2009. Since the mixes had a high SiO_2 content, this allowed for vitrification and a reduction in the water absorption of the aggregate. All of the produced artificial LWAs were within the acceptable limit in terms of water absorption ability, according to the standard. The POFA content level positively influenced the viscosity, which made the surface vitrified. Samples P0S10, P1S9, and P2S8 had high water absorption levels. This result was due to the low isolated surface, with more open pores on the surface, which increased the absorption rate. At 1150 °C, the water absorption decreased as the POFA content increased. This result was due to the formation of the glassy texture on the surface of artificial LWA. Therefore, the amount of water absorption for porous artificial LWA was lessened. The water absorption for sintered artificial LWA depended on the formation of a porous surface and glassy texture in the mixture. Sintered LWA had isolated open pores to limit the access of water through it. The sample with isolated pores and a vitrified matrix surface had a reduced absorption ability. Sample P6S4, with 60% activated POFA, had a low water absorption capacity (5.59%). It had an effective impermeable function, allowing the water to access the aggregate. The reduction in the accessibility of water through the surface connected to the interior porosity was due to its vitrified surface, with a glassy film. The dense external shell and impervious surface of P6S4 resulted in a reduction in the water absorption rate because the pores were sealed by the glassy phase.

By contrast, the sample with an open pore volume tended to absorb more water, given that it was affected by the open pore volume on the external surface [4]. Thus, the water absorption of the artificial LWA was not fully revealed through the SEM microstructure (interior pore size and number). If the open pore volume on the exterior surface area was lower, the water absorption rate was low, but the core region was porous. The analysis of the external surface showed that a cohesion of surface particles occurred. However, more open pores were left on the shell surface if a viscous layer with a lower viscosity existed to allow more gases to escape. With the addition of CaO, the water absorption for artificial LWA significantly decreased. The lime present on the geopolymer POFA reduced the percentage of water absorption.

Figure 6 shows the void percentage for the artificial LWA. An increasing trend in the void percentage was observed for samples P0S10 to P5S5. The void percentage indicated

the change in porosity or pores, which led to the change in density. The void percentage increased as the portion of activated POFA increased. The viscosity of the highly activated POFA sample mixture increased at the same sintering temperature. This was due to the occurrence of bloating behaviour within the artificial LWA. The microstructure of the samples also contributed to this effect, given that more voids formed from the fusion of particles.

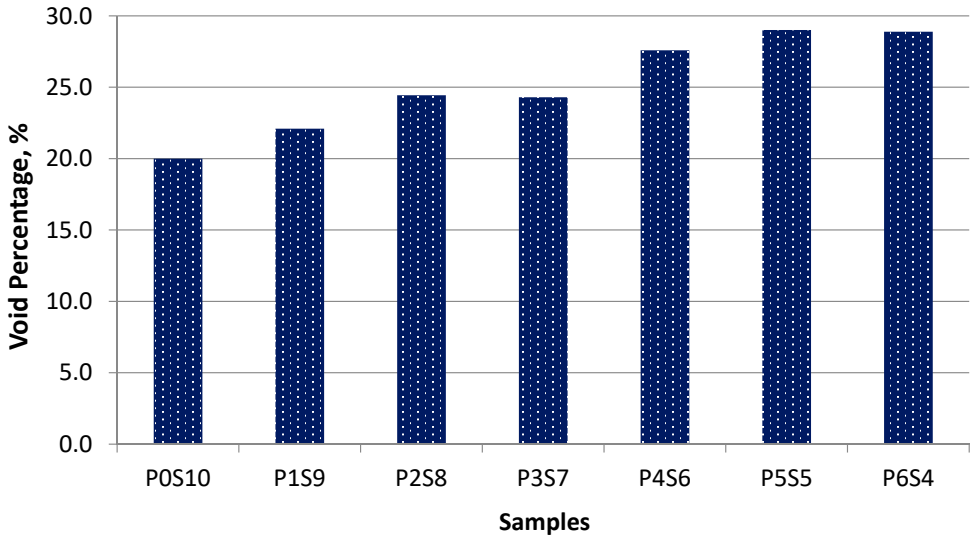

Figure 6. Void percentage for each activated POFA-silt artificial LWA.

3.2. Ignition Loss and BI

In this work, the weight loss percentage of artificial aggregate, before and after sintering, was known as the ignition loss of artificial aggregate. In the process of sintering, the weight loss was most probably due to the evaporation of the water content within the aggregate, the decomposition of the inorganic salt present in the mixture materials, and the emission or oxidation of the organic substances. The presence of highly powdered metallic aluminium encouraged the formation of an aluminium hydroxide $Al(OH)_3$ gel with water, which was revealed by the mass loss of the aggregate. However, the formation of $Al(OH)_3$ caused swelling. Therefore, the crack and fractures in the hardened aggregate could be prevented during preheating in the sintering process.

The LOI of the artificial LWA is shown in Figure 7. Sample P0S10 had a low LOI. Silt is rich in SiO_2 and low in CaO. Thus, the fully silt artificial LWA was less porous and harder to vitrify at the desirable sintering temperature. The low LOI value resulted in less void formation within the artificial LWA. The convection of the elements within silt occurred when the relevant temperature was reached. A vitrified matrix was not formed for sample P0S10. Thus, the released gas escaped, instead of being trapped within the aggregate. The presence of POFA contributed to the increasing trend of LOI. The size of the artificial LWA also reduced as the BI decreased. When the activated POFA increased, the internal and external parts of the artificial LWA were glassy. Sample P6S4 showed a slight decrease in LOI. The reason was that the released gas was trapped within the vitrified surface of the aggregate, and the presence of melted particles filled the interior voids during the sintering process.

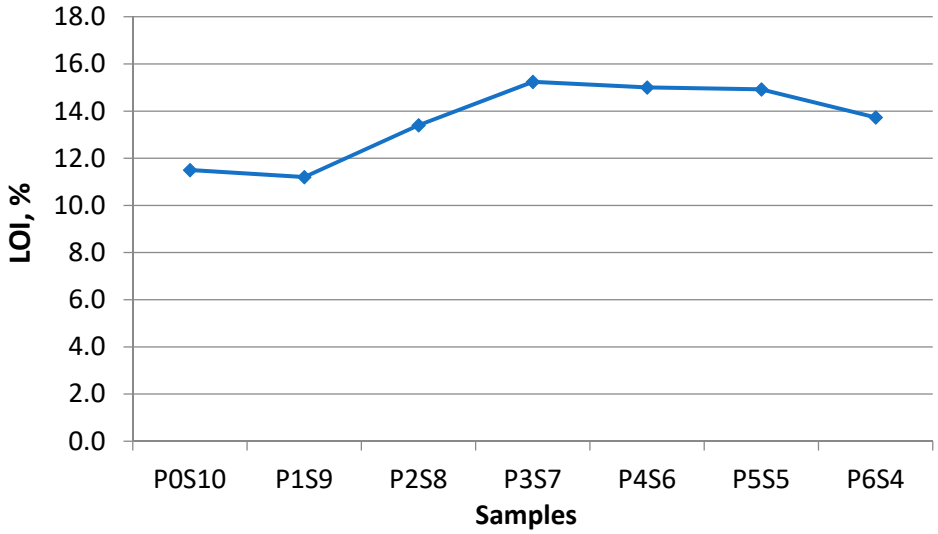

Figure 7. LOI of artificial LWA for different mix ratios.

The density loss of the artificial aggregate is related to the amount of gas that escaped during the sintering process. In this study, the bloating behaviour did not necessarily reflect the release of gas into atmosphere. This phenomenon was due to the influence of released gas after the formation of a viscous layer, as mentioned before. The results in this study evidenced that some of the generated gas for viscous layer formation escaped into the atmosphere and formed tiny pores without effective bloating for artificial LWA. The viscous glass phase was produced simultaneously to encapsulate the released gases, which contributed to the formation of an internal micro-pore structure. Figure 8 shows that all mixes of artificial LWA were classified as expanded aggregates, given that the BI was more than 1. The bloating behaviour was based on the chemical composition of the raw material to form a glassy phase by wrapping gas or the gas generated in the glassy phase [17]. Some samples had a high BI, because more gases were generated and trapped by the viscous melt as the sintering temperature reached 1150 °C. Different proportions of raw materials in the mixture induced changes in the BI. The high content of chemical composition (within the expansion area in the Riley ternary diagram) allowed the materials to expand and trap the released gas. The sintering temperature, released gas, and plastic phase, with the appropriate viscosity to trap the released gases, were run simultaneously [33]. The BI result, illustrated in Figure 8, showed the effect of raw materials on the degree of BI. As the proportion of POFA increased, the BI decreased. The reason was the occurrence of vitrification, which made the structure within the artificial LWA dense. This finding was supported by the study of González-Corrochano et al. [34], which indicated that the raw materials affect the vitrification and mechanical performance of aggregate.

The water absorption of artificial LWA remarkably dropped as the BI increased [28]. This result was due to the formation of a glassy external layer in the pellets, which drastically reduced the permeability of the LWA. The result in Figure 8 showed that the BI and water absorption were correlated with each other. Sample P0S10 had a BI of 2.88, and the BI was 4.43 for sample P6S4. The water absorption exhibited a declining trend from 13.10% (sample P0S10) to 5.59% (sample P6S4). The artificial LWA sintered under a high temperature involved a thermal shock to form a viscous mineral matrix for trapping the formation of evolved gases [35]. At a sintering temperature of 1150 °C, the sufficiently high temperature allowed the surface of the artificial LWA to be vitrified and envelop the emitted gas.

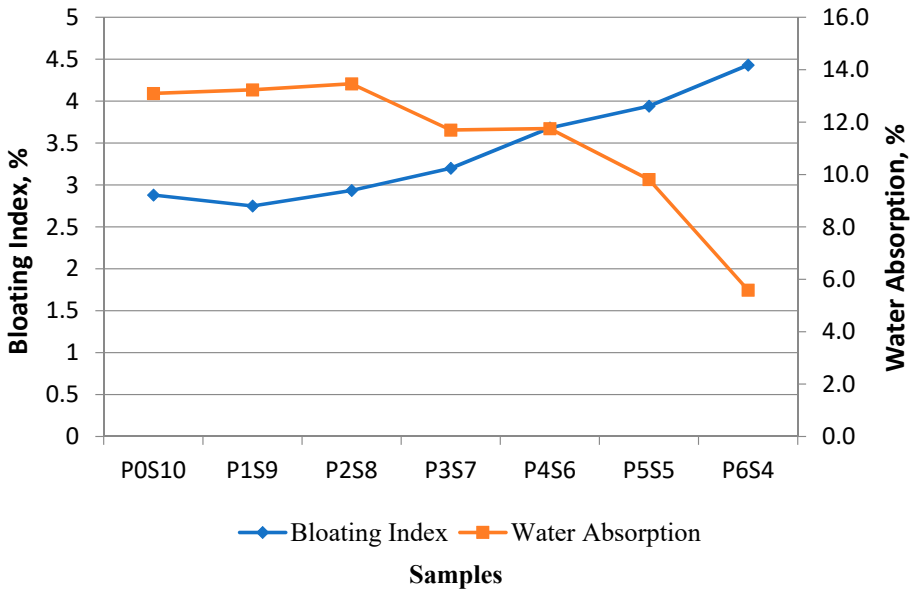

Figure 8. Relationship between BI and water absorption at different mix ratios of artificial LWA.

The activated POFA containing Na_2O exhibited a high BI. This result could be explained by the low melting point in the presence of Na_2O at the sintering temperature [32] and as the proportion of the activated POFA increased. Therefore, this phenomenon could lead to a rapid sintering reaction. As for the proportion of activated POFA up to 70%, the sample was melted in the pre-experiment. The high proportion of activated POFA increased the viscosity and thus encapsulate the bloating gases.

The presence of Fe_2O_3 in the aggregate decomposed during the sintering process and liberated gases (O_2 or SO_2). These released gases probably reacted with the unburned carbon content in the activated POFA to form carbon oxide. A sintering temperature above 1050 °C promoted the generation of liquid and crystal phases. The chemical compositions of SiO_2 and Al_2O_3 that controlled the viscosity of artificial LWA at high temperatures determined the crystalline quality and the crystallisation rate. Thus, the properties of artificial LWA were affected by the chemical oxide in the sintering process [36].

3.3. Mechanical Properties

The effect on the crushing strength of artificial aggregate was due to the different mix proportions of the POFA to silt. The average results of each series of samples at 7, 14, 28, 56, and 90 days are shown in Figure 9. The overall trend observed from the results showed that the ultimate strength achieved by P4S6 was 5.43 MPa at 28 days of curing. As expected, the crushing strength of artificial LWA increased as the binder content increased. However, the crushing strength decreased when the POFA content was beyond 50% of the weight. This phenomenon could be due to the activator POFA, which resulted in the formation of a vitrified structure. The fully silt artificial LWA P0S10 exhibited 3.74 MPa at 28 days. This result was due to the silt failing to boost the crushing strength or enhancing the viscosity without a supporting binder. The crushing strength was also correlated with the BI and density. Whether the formation of the microstructure could withstand the resistance was unclear. A decreasing trend was observed for samples P5S5 and P6S4, which did not explain why the great vitrification enhanced the strength of the aggregate. This result could be explained by the fact that the chemical composition affected the crushing strength of the artificial LWA due to the lower resistance of the internal microstructure. The minimum crushing value (3.7MPa) was 69% of the maximum value (5.4 MPa). Therefore, properties apart from the density, water absorption, morphology of hydration products, and resulting microstructure would also strongly affect the mechanical performance of the artificial LWA. The increase in the activated POFA content modified the densification behaviour of the

mixture, which changed the softening point and sintering temperature with the change in the chemical composition and mineralogy of the mixture. The commercially available LWA has a density of 1.485, a water absorption of 15.5%, and a crushing strength value of 6.9 MPa [37]. Therefore, the crushing strength of the artificial LWA was affected by some interrelated factors, including the density value, shape, size dimension, texture, water absorption (pore distribution and size), BI, and densification of the aggregate.

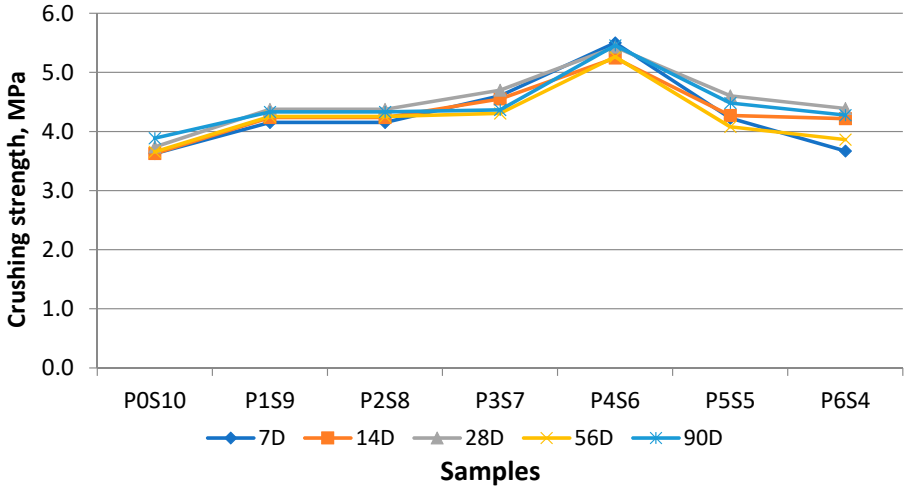

Figure 9. Crushing strength for various mix ratios of artificial LWA at different curing ages.

In general, the artificial LWA with more pores resulted in a low crushing strength. In this study, a good strength was observed for sample P4S6. The reason might be that the formation of pores within the interior of the LWA was closed (not fused) and had a relatively consistent distribution. In addition, the presence of a glassy phase contributed to the crushing strength due to the presence of silicate glass and calcium silicate on the external layer. The appearance, such as the texture of the artificial LWA and pore volume, might affect the bond strength within the cement–aggregate phase. However, the effect would be evident in the early stage of the curing. Thus, the effect in the later stage would be less significant due to the formation of a strong chemical bond.

A good correlation exists between the crushing and impact value for artificial LWA, which can be used to determine the performance of the aggregate. In general, the crushing and impact value provide a full understanding of the strength of the artificial LWA. A high percentage of the impact value indicates that the aggregate has a lower resistance to sudden impacts. The results for each of the samples are presented in Figure 10. As observed, the impact resistance improved as the activated POFA ratio increased. This finding was due to the enhancement in the cement–aggregate bond as a result of the C–S–H formation. The further reaction of the chemical compound in silt and CaO in activated POFA increased the strength. Sample P4S6 had an impact resistance of 24.9%. Samples P5S5 and P6S4 had a slight increment. This result might be because the excessively activated POFA made CaO abundant, which resulted in particles not being reacted because of the rapid hardening process. Samples P3S7 to P6S4 displayed an impact value positioned within the acceptable impact limit, as per BS-812-12. By contrast, the impact value of samples P0S10 to P2S8 did not fall within the impact limit after 28 days of curing. The analysis of the crushing strength and impact value showed that a dense matrix and low water absorption positively contributed to the mechanical performance of the artificial LWA.

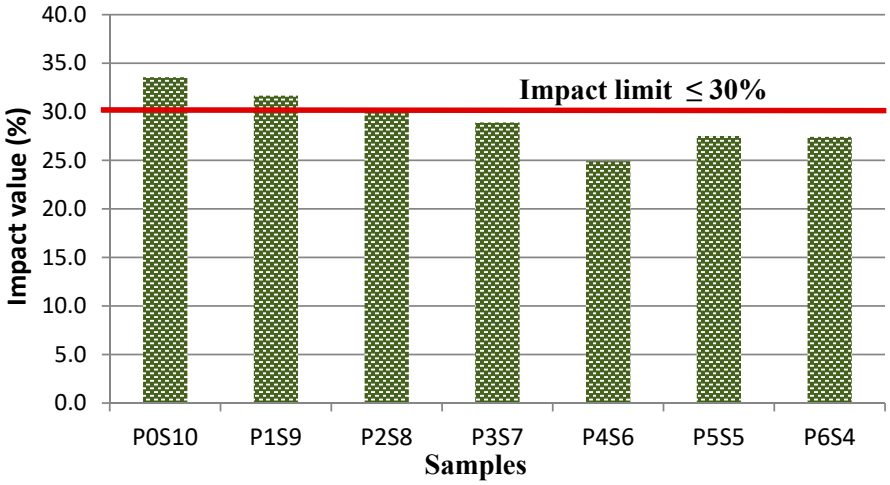

Figure 10. Impact value for various mix ratios of artificial LWA.

The chemical soundness of the artificial LWA was determined according to the standard IS 2386-Part 5 to investigate the resistance of artificial LWA under a magnesium sulphate solution (assumed weathering condition) [38]. The method to run this test was stated in the previous section. The loss of soundness was interrelated to the absorption. The result showed that sample P0S10 had a 4.1% weight reduction, and the value was 0.2% for sample P6S4. The remaining samples obtained 2.5%, 1.1%, 0.9%, 0.7%, and 0.5%. The values of all the samples fell within the limit range of less than 12%, as recommended in ASTM C-88 [39]. Therefore, the samples of artificial LWA had an acceptable loss of soundness to resist changes in volume under the subjected condition.

3.4. The SEM Microstructure of Artificial Aggregate

The microstructures of the internal section of the artificial LWA at varying proportions of POFA-silt were determined by SEM. The dry particle density, water absorption, and crushing strength could be correlated with the microstructure of the artificial LWA. The internal microstructure of LWA was nearly similar for those within the strength range, even with different raw materials or production methods [34]. The artificial LWA showed a dense matrix that contained a significant volume of isolated pores, as the activated POFA content increased. The pore size and void arrangement were affected by the proportion of the mixture for artificial aggregate production. This formation occurred due to the vapor evaporation, oxidation of organic substances, and de-carbonation during the sintering process, and it depended on the mix proportion for artificial LWA production.

Figure 11 shows the change in the microstructure of samples with different proportions at the sintering temperature. Condensed pores, vitrified layers, isolated pores, enlarged pores, or coating melts were formed in the outer and interior parts of the artificial LWA. The SEM morphology of samples **a** (P0S10) and **b** (P1S9) showed a nearly similar structure with abundant small voids and a few large pores. No glassy layer was formed in the core fragment morphology. Thus, sample **a** (P0S10) failed to trap the expanded gas. Sample **a** (P0S10) had fewer and finer pores in the fractured core. The pores were not interconnected and did not expand. This sample also had a glossy and smooth inner pore surface. The interior of the samples appeared to be not fully vitrified/bloating. This result was due to the gas causing decomposition reactions in a glassy matrix of a low viscosity. The sample with a low water absorption consisted of closed pores inside the compound matrix. The microparticles of **b** (P1S9) started to slightly expand, but the expansion was limited.

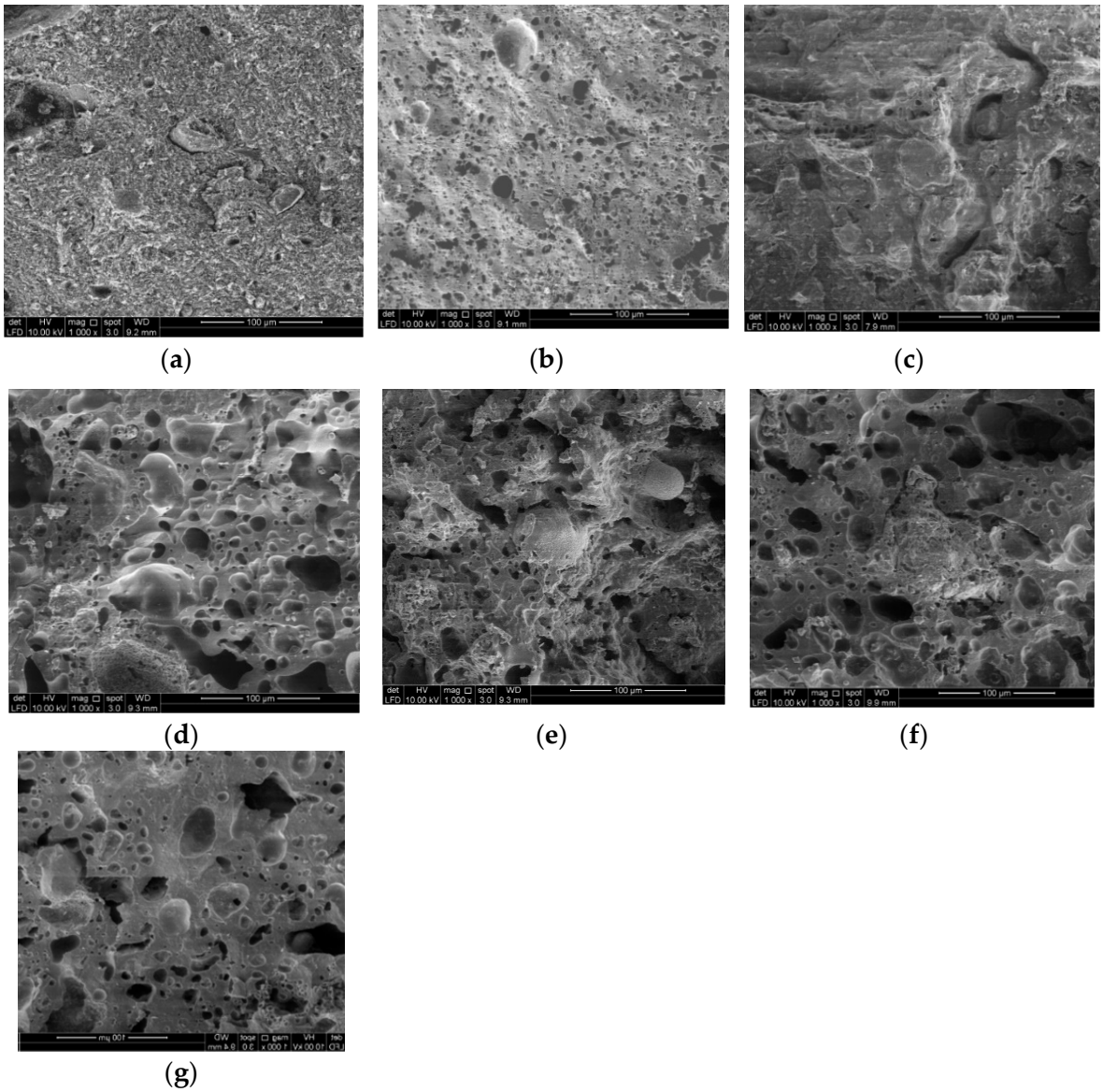

Figure 11. SEM image of artificial LWA derived from activated POFA-silt at different ratios under 1000× magnification, (**a**) P0S10; (**b**) P1S9; (**c**) P2S8; (**d**) P3S7; (**e**) P4S6; (**f**) P5S5; (**g**) P6S4.

As the proportion of activated POFA increased, the pores eventually expanded due to the low viscosity to withstand the bloating force from the released gas. This internally generated an isolated void, followed by a softened phenomenon. The enlargement of pores was attributed to the vapor entrapment derived from the generated gas from the viscous composition within the artificial LWA. An obvious volatilisation was observed in sample **d** (P3S7) to **f** (P5S5). The artificial LWA started to develop a glassy layer, with a notable void formation. When the proportion of POFA content increased, a large void existed and was surrounded by a glassy layer. The raw POFA contained higher CaO and MgO contents than silt. Thus, the sintering temperature stimulated a sudden change in viscosity. The formation of large pores was followed by a glassy phase. Sample **g** (P6S4) gained the external glassy film, which resulted in a low water absorption. The continuous viscous phase during the sintering process decreased or broke the void to form an interconnection within the aggregate and thus affected the strength of the artificial LWA. Therefore, the higher amount of isolated spherical pores in the fractured cores and the thicker inter-pore crystalline phases affected the artificial LWA with a high activated POFA content. For sample **g** (P6S4), the formation of the large void was distorted without the glassy wall. The

viscosity to capture the expanded gas was limited, and the sample was nearly or partially melted. The bloating effect and fusing occurred in the activated POFA at 1150 °C. As the ratio of activated POFA increased, the portion to be expanded was easily detected in the microstructure image. The sample with 70% POFA melted at the sintering temperature of 1150 °C. This phenomenon occurred because the chemical composition of the aggregate mixture reached its melting point.

The presence of lime in POFA acted as a stabiliser with silt and further reacted with the silicate in POFA and silt to form a stronger binder or cement of the calcium silicate and aluminate hydrate. This substance was produced when the hydration process was formed.

3.5. X-ray Diffraction of Artificial Aggregate

The X-ray diffraction (XRD) analysis results are shown in Figure 12. The major crystalline phase presence is quartz (SiO_2) for all the samples, where the artificial LWA exhibited an amorphous characteristic. The property of raw material for the artificial aggregate production contributed to the major prominent oxide, since it contained a high SiO_2 content. For sample P0S10, the crystalline phases performed included quartz, illite, microcline, and muscovite. Sample P1S9 consisted of quartz, cristobalite, diopside, and jacobsite. The mullite present had a low coefficient of the thermal expansion, which allowed for less expanded gas to form in the artificial LWA. The crystalline phases of quartz, oligoclase, hermatile, titanomagnetite, and manganese were found in sample P2S8. FeO was not observed, since there was no wuestite phase in the XRD pattern. Moreover, sample P3S7 illustrated quartz, oligoclase, hermatile, magnesioferrite, and kyanite. Kyanite is an anhydrous aluminosilicate, and it is detected at 1150 °C sintering for aggregate samples with more than 30% POFA. The presence of kyanite contributed to the compressive strength, as it compromised the crushing strength for artificial LWA. The mineral phase present in sample P5S5 was almost similar to that of sample P4S6. Sample P4S6 had crystalline phases of quartz, oligoclase, siderite, and kyanite. With the incorporation of activated POFA, the C-S-H formation was enhanced, which was in agreement with the crushing strength. Sample P6S4 detected a rose in the quartz intensity due to the formation of a glassy phase during the sintering process.

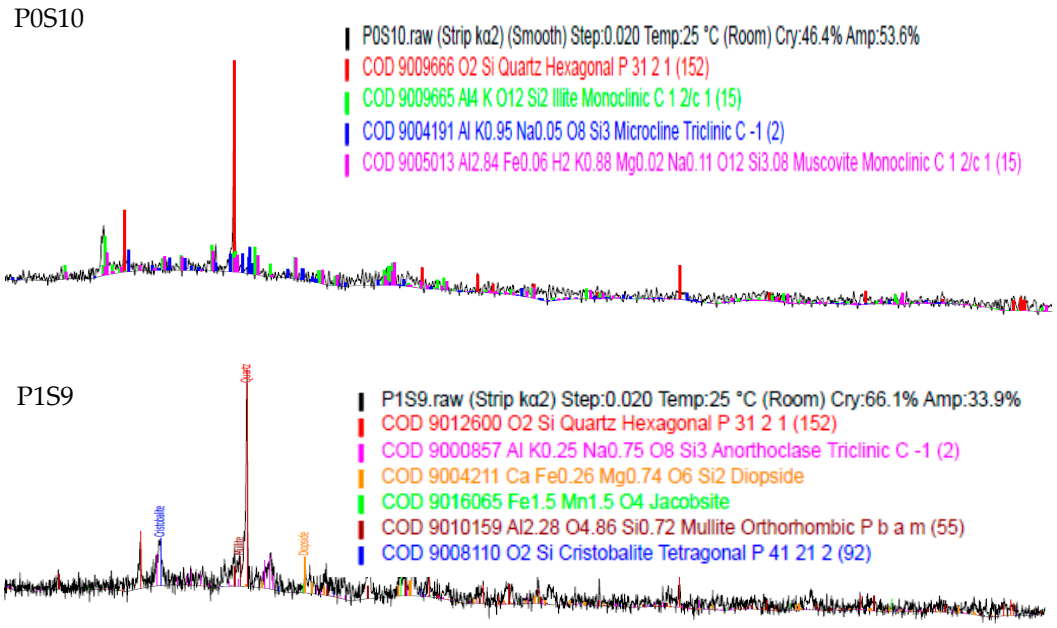

Figure 12. *Cont.*

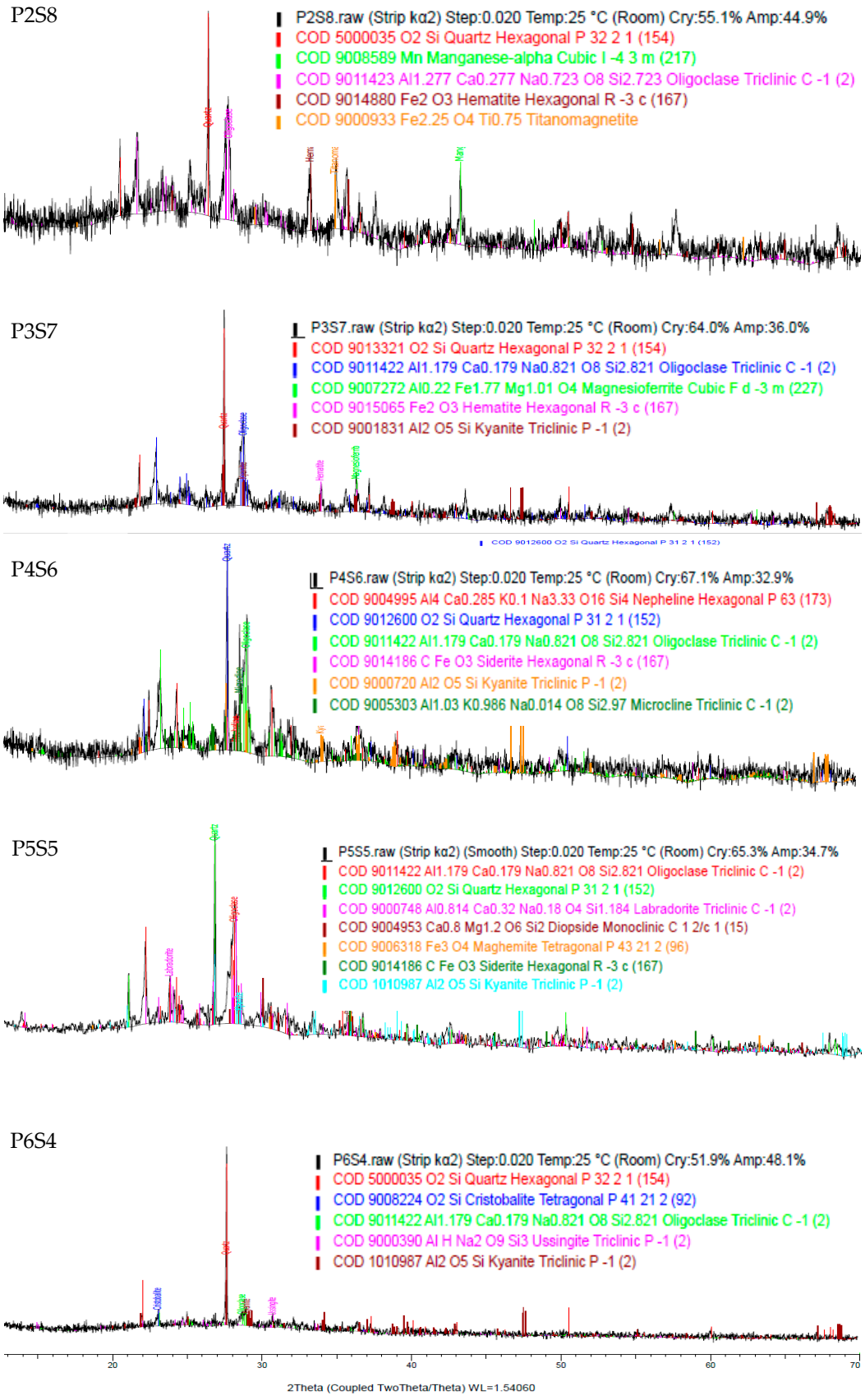

Figure 12. XRD of artificial LWA at various mix proportion ratios.

4. Conclusions

The use of by-product residues of POFA and unwanted sludge as artificial LWA is not only useful in exploring alternatives to natural aggregate, but also provides a solution for waste management through the recycling and reuse of wastes. The general properties of the raw materials show that it is highly likely that they can be used to generate artificial LWA. This study demonstrated that activated POFA-silt could be used to manufacture artificial LWA through the cementitious granulation of POFA geopolymer. The performance of the combination of sintered POFA-silt artificial LWA was evaluated. The results showed that alkaline-activated POFA with silt could be used for artificial LWA production. The physical, mechanical, and durability properties of artificial POFA-silt LWA sintered at 1150 °C were determined. The findings are as follows:

(1) All of the mix proportions of artificial LWA were in accordance with the standard in terms of density and water absorption. Each of the artificial LWAs had different trends, which were all within the limit range.
(2) The use of lime (CaO) in POFA produced a pozzolanic material through a chemical reaction with the silicate mineral in POFA. When it was combined with silt, a hydration process occurred due to the presence of CaOH, silicate, and aluminate in the silt, which caused a binder of calcium silicate or aluminate hydrate to form, thus enhancing the reaction in the artificial LWA.
(3) Waste materials with high SiO_2, Al_2O_3, and CaO contents, such as silt and POFA, had a high potential to be manufactured as artificial aggregates with the addition of additives, which is due to the formation of a C-S-H gel or Na-Al-H gel during the reaction. SiO_2 and Al_2O_3 mainly controlled the viscosity of the glassy phase. These materials affected the properties of the artificial aggregates, such as their bulk density, particle density, and water absorption.
(4) The bulk and particle densities of the artificial LWA were consistent with the requirement of LWA. Thus, all of the POFA-silt artificial aggregates were classified as LWA. The water absorption of the artificial aggregates was considered acceptable. The reason was that a vitrified external layer formed in all samples, with a better ratio of activated POFA.
(5) Sample P4S6 exhibited a satisfactory performance in the property tests. The physical properties fell within the requirement. It achieved the highest strength in terms of single aggregate crushing. Sample P4S6 was a good optimal mix proportion for artificial LWA production. This artificial LWA could be applied to concrete slabs and building structures. It could also be used for lightweight structures or insulation concrete to fulfil the need for high-strength and lightweight concrete.
(6) The chemical mineralogy of the raw materials in different proportions for artificial LWA production affected the pore formation within the artificial LWA and the degree of vitrification.
(7) The slightly abnormal performance of the artificial LWA might be due to the sintering process. The location of the aggregate induced changes in the texture, causing it to be either well vitrified or less vitrified. This phenomenon occurred because of the circulation of heat inside the furnace, which failed to completely reach each stationary artificial LWA.

This work could serve as a reference in material waste recycling or reuse and recovery. The developed material could be used as an alternative to address the overconsumption of natural aggregate. It could also be a feasible solution for industrial waste management. The artificial LWA could be manufactured in large amounts to reduce costs and energy consumption. Thus, further investigations could be conducted to explore more related possibilities, such as other potential geopolymer sources, the addition of admixture or superplasticiser, and more efficient production methods.

Author Contributions: Conceptualization, S.Y.K. and H.A.; methodology, S.Y.K. and H.A.; analysis, S.Y.K.; writing—original draft preparation, S.Y.K.; writing—review and editing, H.A.; supervision, H.A. All authors have read and agreed to the published version of the manuscript.

Funding: This research was funded by the Ministry of Higher Education of Malaysia under the Fundamental Grant, No: 203/PPBGN/6711610.

Institutional Review Board Statement: Not applicable.

Informed Consent Statement: Not applicable.

Data Availability Statement: Not applicable.

Acknowledgments: The authors gratefully acknowledge the financial support of the Ministry of Higher Education of Malaysia under the Fundamental Grant, No: 203/PPBGN/6711610.

Conflicts of Interest: The authors have no conflict of interest to declare that are relevant to the contents of this article.

References

1. Allen, E.; Iano, J. *Fundamentals of Building Construction: Materials and Methods*, 5th ed.; John Wiley & Sons, Inc.: New York, NY, USA, 2008.
2. Mehta, P.K.; Monteiro, P.J. *Concrete: Microstructure, Properties, and Materials*; McGraw-Hill Education: Berkshire, UK, 2014.
3. Ismail, A.; Samad, M.H.A.; Rahman, A.M.A.; Yeok, F.S. Cooling potentials and CO_2 uptake of Ipomoea Pes-caprae installed on the flat roof of a single storey residential building in Malaysia. *Procedia Soc. Behav. Sci.* **2012**, *35*, 361–368. [CrossRef]
4. Hainin, M.R.; Yusoff, N.I.M.; Mohammad Sabri, M.F.; Abdul Aziz, M.A.; Sahul Hameed, M.A.; Farooq Reshi, W. Steel slag as an aggregate replacement in Malaysian hot mix asphalt. *Int. Sch. Res. Not.* **2012**, *2012*. [CrossRef]
5. Haron, Z. Design of One Way Reinforced Concrete Element to Resist the Effects of an Accidental Explosion. Ph.D. Thesis, Universiti Teknologi Malaysia, Skudai, Malaysia, 1993.
6. Huang, C.; Pan, J.R.; Liu, Y. Mixing water treatment residual with excavation waste soil in brick and artificial aggregate making. *J. Environ. Eng.* **2005**, *131*, 272–277. [CrossRef]
7. Lau, P.; Teo, D.; Mannan, M. Characteristics of lightweight aggregate produced from lime-treated sewage sludge and palm oil fuel ash. *Constr. Build. Mater.* **2017**, *152*, 558–567. [CrossRef]
8. Breesem, K.M.; Faris, F.G.; Abdel-Magid, I.M. Reuse of alum sludge in construction materials and concrete works: A general overview. *Infrastucture Univ. Kuala Lumpur Res. J.* **2014**, *2*, 20–30.
9. Xu, Y.; Yan, C.; Xu, B.; Ruan, X.; Wei, Z. The use of urban river sediments as a primary raw material in the production of highly insulating brick. *Ceram. Int.* **2014**, *40*, 8833–8840. [CrossRef]
10. Benlalla, A.; Elmoussaouiti, M.; Dahhou, M.; Assafi, M. Utilization of water treatment plant sludge in structural ceramics bricks. *Appl. Clay Sci.* **2015**, *118*, 171–177. [CrossRef]
11. Wolff, E.; Schwabe, W.K.; Conceição, S.V. Utilization of water treatment plant sludge in structural ceramics. *J. Clean. Prod.* **2015**, *96*, 282–289. [CrossRef]
12. Adam, N.A.; Sulaiman, A.; Baharuddin, A.S.; Mokhtar, M.N.; Busu, Z.; Mulok, T.E.T.Z. Synthesis and characterisation of silica from palm oil fuel ash (POFA) using alkaline fusion method. *Pertanika J. Sci. Technol.* **2017**, *25*, 269–279.
13. Alnahhal, M.F.; Alengaram, U.J.; Jumaat, M.Z.; Alqedra, M.A.; Mo, K.H.; Sumesh, M. Evaluation of industrial by-products as sustainable pozzolanic materials in recycled aggregate concrete. *Sustainability* **2017**, *9*, 767. [CrossRef]
14. Yap, S.; Alengaram, U.; Jumaat, M.; Foong, K. Waste materials in Malaysia for development of sustainable concrete: A review. *Electron. J. Struct. Eng.* **2013**, *13*, 60–64.
15. Khalid, N.; Arshad, M.F.; Mukri, M.; Kamarudin, F.; Ghani, A.H.A. The California bearing ratio (CBR) value for banting soft soil subgrade stabilized using lime-pofa mixtures. *Electron. J. Geotech. Eng.* **2014**, *19*, 155–163.
16. Alrshoudi, F.; Mohammadhosseini, H.; Alyousef, R.; Alghamdi, H.; Alharbi, Y.R.; Alsaif, A. Sustainable use of waste polypropylene fibers and palm oil fuel ash in the production of novel prepacked aggregate fiber-reinforced concrete. *Sustainability* **2020**, *12*, 4871. [CrossRef]
17. Moreno-Maroto, J.M.; Cobo-Ceacero, C.J.; Uceda-Rodríguez, M.; Cotes-Palomino, T.; García, C.M.; Alonso-Azcárate, J. Unraveling the expansion mechanism in lightweight aggregates: Demonstrating that bloating barely requires gas. *Constr. Build. Mater.* **2020**, *247*, 118583. [CrossRef]
18. Zarina, Y.; Mohd Mustafa, A.B.A.; Kamarudin, H.; Khairul Nizar, I.; Andrei Victor, S.; Petrică, V.; Rafiza, A.R. Chemical and Physical Characterization of Boiler Ash from Palm Oil Industry Waste for Geopolymer Composite. 2013. Available online: http://dspace.unimap.edu.my/xmlui/handle/123456789/41480 (accessed on 6 June 2013).
19. Nadziri, N.; Ismail, I.; Hamdan, S. Binding gel characterization of alkali-activated binders based on palm oil fuel ash (POFA) and fly ash. *J. Sustain. Cem. Mater.* **2018**, *7*, 1–14. [CrossRef]

20. Zarina, Y.; Mohd Mustafa Al Bakri, A.; Kamaruddin, H.; Nizar, K.; Rafiza, A.R. Review on the various ash from palm oil waste as geopolymer material. *Rev. Adv. Mater. Sci.* **2013**, *34*, 37–43. Available online: http://dspace.unimap.edu.my/dspace/handle/123456789/36152 (accessed on 9 September 2012).
21. Salami, B.A.; Johari, M.A.M.; Ahmad, Z.A.; Maslehuddin, M. POFA-engineered alkali-activated cementitious composite performance in acid environment. *J. Adv. Concr. Technol.* **2017**, *15*, 684–699. [CrossRef]
22. Kaur, K.; Singh, J.; Kaur, M. Compressive strength of rice husk ash based geopolymer: The effect of alkaline activator. *Constr. Build. Mater.* **2018**, *169*, 188–192. [CrossRef]
23. Singh, G.B.; Subramaniam, K.V. Evaluation of sodium content and sodium hydroxide molarity on compressive strength of alkali activated low-calcium fly ash. *Cem. Concr. Compos.* **2017**, *81*, 122–132. [CrossRef]
24. Salami, B.A.; Johari, M.A.M.; Ahmad, Z.A.; Maslehuddin, M. Durability performance of palm oil fuel ash-based engineered alkaline-activated cementitious composite (POFA-EACC) mortar in sulfate environment. *Constr. Build. Mater.* **2017**, *131*, 229–244. [CrossRef]
25. Salami, B.A.; Johari, M.A.M.; Ahmad, Z.A.; Maslehuddin, M.; Adewumi, A.A. Impact of Al(OH)3 addition to POFA on the compressive strength of POFA alkali-activated mortar. *Constr. Build. Mater.* **2018**, *190*, 65–82. [CrossRef]
26. Kaur, M.; Singh, J.; Kaur, M. Microstructure and strength development of fly ash-based geopolymer mortar: Role of nano-metakaolin. *Constr. Build. Mater.* **2018**, *190*, 672–679. [CrossRef]
27. Lin, C.F.; Wu, C.H.; Ho, H.M. Recovery of municipal waste incineration bottom ash and water treatment sludge to water permeable pavement materials. *Waste Manag.* **2006**, *26*, 970–978. [CrossRef]
28. González-Corrochano, B.; Alonso-Azcárate, J.; Rodríguez, L.; Lorenzo, A.P.; Torío, M.F.; Ramos, J.J.T.; Muro, C. Valorization of washing aggregate sludge and sewage sludge for lightweight aggregates production. *Constr. Build. Mater.* **2016**, *116*, 252–262. [CrossRef]
29. Tasnim, S.; Rahman, M.E.; Ahmadi, R.B. Mechanical performance of modified cement paste made with micro-fine POFA in ammonium nitrate environment. *Constr. Build. Mater.* **2018**, *162*, 534–542. [CrossRef]
30. González-Corrochano, B.; Alonso-Azcárate, J.; Rodas, M. Production of lightweight aggregates from mining and industrial wastes. *J. Environ. Manag.* **2009**, *90*, 2801–2812. [CrossRef]
31. Wei, Y.L.; Lin, C.Y.; Ko, K.W.; Wang, H.P. Preparation of low water-sorption lightweight aggregates from harbor sediment added with waste glass. *Mar. Pollut. Bull.* **2011**, *63*, 135–140. [CrossRef]
32. Tuan, B.L.A.; Hwang, C.L.; Lin, K.L.; Chen, Y.Y.; Young, M.P. Development of lightweight aggregate from sewage sludge and waste glass powder for concrete. *Constr. Build. Mater.* **2013**, *47*, 334–339. [CrossRef]
33. Yang, C.; Cui, C.; Qin, J. Recycling of low-silicon iron tailings in the production of lightweight aggregates. *Ceram. Int.* **2015**, *41*, 1213–1221. [CrossRef]
34. González-Corrochano, B.; Alonso-Azcárate, J.; Rodas, M.; Luque, F.; Barrenechea, J. Microstructure and mineralogy of lightweight aggregates produced from washing aggregate sludge, fly ash and used motor oil. *Cem. Concr. Compos.* **2010**, *32*, 694–707. [CrossRef]
35. Moreno-Maroto, J.M.; González-Corrochano, B.; Alonso-Azcárate, J.; Rodríguez, L.; Acosta, A. Development of lightweight aggregates from stone cutting sludge, plastic wastes and sepiolite rejections for agricultural and environmental purposes. *J. Environ. Manag.* **2017**, *200*, 229–242. [CrossRef]
36. Pourakbar, S.; Asadi, A.; Huat, B.B.; Fasihnikoutalab, M.H. Stabilization of clayey soil using ultrafine palm oil fuel ash (POFA) and cement. *Transp. Geotech.* **2015**, *3*, 24–35. [CrossRef]
37. Adell, V. *Production of Lightweight Aggregate from Problematic Waste Ashes Using the Lytag Process*; Department of Civil and Environmental Engineering, Imperial College London: London, UK, 2007.
38. Sharma, A.K.; Anand, K. Comparative study on synthesis and properties of geopolymer fine aggregate from fly ashes. *Constr. Build. Mater.* **2019**, *198*, 359–367. [CrossRef]
39. Haynes, H. ASTM C 88 Test on soundness of aggregate using sodium sulfate or magnesium sulfate: A study of the mechanisms of Damage. *J. ASTM Int.* **2005**, *2*, 1–17. [CrossRef]